

ORIGINAL
RESEARCH

S.J. Mills
C. Soh
J.P.B. O'Connor
C.J. Rose
G. Buonaccorsi
S. Cheung
S. Zhao
G.J.M. Parker
A. Jackson



Enhancing Fraction in Glioma and Its Relationship to the Tumoral Vascular Microenvironment: A Dynamic Contrast-Enhanced MR Imaging Study

BACKGROUND AND PURPOSE: EnF is a newly described measure of proportional tumor enhancement derived from DCE-MR imaging. The aim of this study was to assess the relationship between EnF and the more established DCE-MR imaging parameters: K^{trans} , v_e , and v_p .

MATERIALS AND METHODS: Forty-two patients with 43 gliomas (16 grade II, 3 grade III, and 24 grade IV) were studied. Imaging included pre- and postcontrast T1-weighted sequences through the lesion and T1-weighted DCE-MR imaging. Parametric maps of EnF, K^{trans} , v_e , and v_p were generated. Voxels were classified as enhancing if the IAUC was positive ($EnF_{IAUC60>0}$). A threshold of IAUC > 2.5 mmol.s was used to generate $EnF_{IAUC60>2.5}$. Both measures of EnF were compared with the DCE-MR imaging parameters (K^{trans} , v_e , and v_p).

RESULTS: In grade II gliomas, $EnF_{IAUC60>0}$ and $EnF_{IAUC60>2.5}$ correlated with v_p ($R^2 = 0.6245$, $P < .0005$; and $R^2 = 0.4727$, $P = .003$) but not with K^{trans} or v_e . In grade IV tumors, both $EnF_{IAUC60>0}$ and $EnF_{IAUC60>2.5}$ correlated with K^{trans} ($R^2 = 0.3501$, $P = .001$; and $R^2 = 0.4699$, $P < .0005$) and v_p ($R^2 = 0.1564$, $P = .01$; and $R^2 = 0.2429$, $P = .007$), but not with v_e . Multiple regression analysis showed K^{trans} as the only independent correlate of both $EnF_{IAUC60>0}$ and $EnF_{IAUC60>2.5}$ for grade IV tumors.

CONCLUSIONS: This study suggests that in grade II tumors, EnF reflects v_p and varies due to changes in vascular density. In grade IV gliomas, EnF is affected by K^{trans} with secondary associated changes in v_p .

ABBREVIATIONS: AIF = arterial input function; DCE-CT = dynamic contrast-enhanced CT; DCE-MR = dynamic contrast-enhanced MR imaging; EnF = enhancing fraction; $EnF_{IAUC60>0}$ = unthresholded enhancing fraction; $EnF_{IAUC60>2.5}$ = thresholded enhancing fraction; IAUC = initial area under the concentration curve; $IAUC_{60}$ = initial area under the concentration curve during the first 60 seconds; K^{trans} = contrast-transfer coefficient; rCBV = relative cerebral blood volume; v_e = extravascular extracellular space volume per unit volume of tissue; VEGF = vascular endothelial growth factor; VOI = volume of interest; v_p = blood plasma volume per unit volume of tissue; WHO = World Health Organization

DCE-MR imaging allows characterization of the vascular microenvironment in tumors by measurement of a range of parameters that reflect specific physiologic characteristics. One of the simplest measures is the IAUC during a given time, usually 60 seconds ($IAUC_{60}$).¹ While IAUC is simple to calculate and has been shown to be a reliable and reproducible parameter,² it has no physiologic specificity. More complex postprocessing analysis uses pharmacokinetic modeling to measure K^{trans} (reflecting both flow and permeability), v_e , v_p ,

and rCBV.³ These complex measures have greater physiologic specificity and relate predictably to various aspects of tumor biology. In gliomas, measures of blood volume, both rCBV and v_p , have demonstrated excellent discrimination of tumor grade,⁴⁻¹⁴ subtype,¹⁵ and genotype^{16,17}; and K^{trans} also discriminates grade.^{13,18-20} Both blood volume and K^{trans} have been identified as prognostic indicators of survival in glioma,²¹⁻²⁵ but unlike blood volume, the relationship between K^{trans} and patient survival is independent of its relationship with histologic grade.²³

Recent investigators studying solid masses of the abdomen have proposed a simple measure of bulk tumor perfusion from DCE-MR imaging, the EnF or perfused proportion,^{26,27} which is the ratio of enhancing to total tumor volume. A CT variant of this measure has shown promise in differentiating stable from progressive disease and in predicting time to progression following first-line chemotherapy in ovarian cancer.²⁸ Measurements of IAUC can be used to reproducibly stratify voxels as enhancing or nonenhancing for a definition of the EnF. Because the IAUC is a continuous variable, the distinction between enhancing and nonenhancing can be defined by the presence of enhancement (IAUC > 0 mmol.s) or by use of a threshold value to define a minimal acceptable level of enhancement. In a previous study, we have demonstrated that EnF defined at a threshold of $IAUC_{60} > 2.5$ mmol.s pro-

Received June 18, 2009; accepted after revision August 22.

From Imaging Science and Biomedical Engineering (S.J.M., J.P.B.O., C.J.R., G.B., S.C., S.Z., G.J.M.P., A.J.), University of Manchester, Manchester, United Kingdom; and Department of Neuroradiology (S.J.M., C.S., A.J.), Hope Hospital, Salford, United Kingdom.

This research was funded by a research training bursary from Cancer Research UK, ref: C21247/A6840. S.J. Mills is funded by a Cancer Research UK Clinicians Training Fellowship, ref: C21247/A7473; J.P.B. O'Connor is funded by a Cancer Research UK Clinicians Training Fellowship, ref: C19221/A6086; G. Buonaccorsi is funded by a Cancer Research UK Program Grant, ref: C237/A6295; and C.J. Rose is funded by GlaxoSmithKline.

Please address correspondence to Samantha Mills, MD, Wolfson Molecular Imaging Centre, Imaging Sciences and Biomedical Engineering, University of Manchester, 27 Palatine Rd, Withington, Manchester, M20 3LJ, United Kingdom; e-mail: samantha.mills@manchester.ac.uk



Indicates open access to non-subscribers at www.ajnr.org

DOI 10.3174/ajnr.A1925

Table 1: Correlation matrix for all parameters in the grade II glioma group and Spearman ρ correlation coefficients for cross-correlations between parameters (with significance levels)

	K^{trans}	v_e	v_p	$EnF_{IAUC60>0}$	$EnF_{IAUC60>2.5}$
K^{trans}	1.000	-0.756 ($P = .001$) ^a	-0.225 ($P = .402$)	-0.025 ($P = .926$)	-0.001 ($P = .996$)
v_e	-0.756 ($P = .001$) ^a	1.000	0.524 ($P = .037$) ^b	0.329 ($v = .213$)	0.097 ($P = .721$)
v_p	-0.225 ($P = .402$)	0.524 ($P = .037$) ^b	1.000	0.838 ($P < .0005$) ^a	0.697 ($P = .003$) ^a
$EnF_{IAUC60>0}$	-0.025 ($P = .926$)	0.329 ($P = .213$)	0.838 ($P < .0005$) ^b	1.000	0.576 ($P = .019$) ^b
$EnF_{IAUC60>2.5}$	-0.001 ($P = .996$)	0.097 ($P = .721$)	0.697 ($P = .003$) ^a	0.576 ($P = .019$) ^b	1.000

^a Correlation is significant at the .01 level (2-tailed).^b Correlation is significant at the .05 level (2-tailed).

vides optimal discrimination between low- and high-grade gliomas.²⁹

The value of EnF in an individual tumor will be affected by a number of variations in the tumor vascular microenvironment. Areas of necrosis or nonperfusion will clearly fail to enhance, but enhancement may also not occur in viable tumor if perfusion pressure and perfusion rates are low relative to the vascular half-life of the contrast media. The specific aim of this study was to investigate the effects of variations in DCE-MR imaging parameters, K^{trans} , v_e , and v_p , on measured EnF in glioma.

Materials and Methods

Patients

The local research ethics committee approved the study, and all patients gave informed consent before recruitment. Patients were identified via the neuro-oncology multidisciplinary team meetings at Salford Royal National Health Service Foundation Trust. All imaging was performed before surgery. All tumors were histologically confirmed as gliomas and graded according to the WHO classification criteria.³⁰ All patients with grade IV tumors received corticosteroid treatment for a minimum of 48 hours before imaging. None received any other form of treatment at the time of imaging or before surgery. Findings in this group of patients describing the differences in EnF between low- and high-grade tumors have been reported previously.²⁹

Data Acquisition

Imaging was performed at the University of Manchester Magnetic Resonance Imaging Facility (Hope Hospital, Salford, United Kingdom) by using a sensitivity encoding head coil on a 3T Achieva system (Philips Medical Systems, Best, the Netherlands). DCE-MR imaging was acquired in a sagittal oblique orientation to incorporate the internal carotid artery for measurement of an AIF. Four precontrast T1 fast-field echo (radio-frequency-spoiled gradient-echo) sequences ($\alpha = 2^\circ, 5^\circ, 10^\circ, \text{ and } 16^\circ$) were acquired in the same geometry for calculation of baseline T1 maps (TR, 3.5 ms; TE, 1.1 ms; section thickness, 4.2 mm; 128×128 ; FOV, $230 \times 230 \times 105$ mm). This was followed by a dynamic contrast-enhanced acquisition series (TR, 3.5 ms; TE, 1.1 ms; flip angle, 16° ; section thickness, 4.2 mm; 128×128 ; FOV, $230 \times 230 \times 105$ mm), consisting of 100 volumes with temporal spacing of approximately 3.4 seconds. Gadolinium-based contrast agent (Gd-DTPA-BMA; Omniscan, GE Healthcare, Oslo, Norway) was injected as a bolus dose of 0.1 mmol/kg^{-1} of body weight, at a rate of 3 mL/s^{-1} , after acquisition of the fifth image volume. Pre- and postcontrast T1-weighted imaging sequences (TR, 9.3 ms; TE, 4.6 ms) were acquired in the same sagittal oblique geometry for definition of the VOI of the whole tumor.

Data Analysis

An experienced radiologist (S.J.M.) manually defined VOIs for each tumor on the postcontrast T1 geometrically matched sequences, drawing around signal intensity abnormality/contrast enhancement by using a technique that has previously shown good interobserver agreement (intraclass correlation coefficient, >0.94),³¹ before histologic diagnosis was confirmed. Postprocessing analysis was performed by using in-house software (Manchester Dynamic Modeling) and the extended Tofts and Kermode pharmacokinetic model.³ Automated AIFs were generated from an appropriately chosen section that included the internal carotid artery.³² Parametric maps of K^{trans} , v_p , v_e , and $IAUC_{60}$ were produced.

For each tumor, $EnF_{IAUC60>0}$ was calculated by dividing the enhancing volume (volume of voxels with an $IAUC_{60}>0 \text{ mmol.s}$) by the total volume of the VOI. $EnF_{IAUC60>2.5}$ was calculated by using a previously identified optimal threshold of $IAUC_{60} (>2.5 \text{ mmol.s})$, above which voxels were considered to be enhancing. This optimized threshold was defined on an initial dataset of 5 grade II and 10 grade IV gliomas to identify the optimum $IAUC_{60}$ threshold for distinguishing histologic grade.²⁹

Statistical Analysis

All statistical analyses were performed by using SPSS, Version 15.0 (SPSS, Chicago, Illinois). Data were not normally distributed; therefore, nonparametric analyses were performed. Tumors were grouped according to grade (II, III, and IV), and grade II tumors were further separated according to histologic subtype (astrocytomas and tumors with an oligodendroglial component). For each tumor grade and histologic subtype of the grade II tumors, scatterplots of median values of the DCE-MR imaging parameters versus $EnF_{IAUC60>0}$ and $EnF_{IAUC60>2.5}$ were generated. Comparison between individual DCE-MR imaging parameters and both $EnF_{IAUC60>0}$ and $EnF_{IAUC60>2.5}$ was performed by using a bivariate Spearman rank correlation analysis for grade II and IV tumors and the 2 histologic subgroups of grade II tumors; there were insufficient numbers in the grade III group to perform this analysis. On finding significant correlations, all parameters were entered into a multiple linear regression analysis by using a forward entry model, with an entry criterion of $P < .05$ to evaluate any cross-correlation between parameters.

Results

We recruited 42 patients: 18 women and 24 men, with a mean age of 49 ± 16 years (range, 19–77 years). There were a total of 43 tumors, because 1 patient had bilateral grade II tumors, each of distinct histologic subtype (astrocytoma and oligodendroglioma). The 16 grade II tumors included 6 astrocytomas (4 diagnosed by biopsy and 2 by surgical debulking), 3 oligoastrocytomas (all surgically debulked), and 7 oligodendroglio-

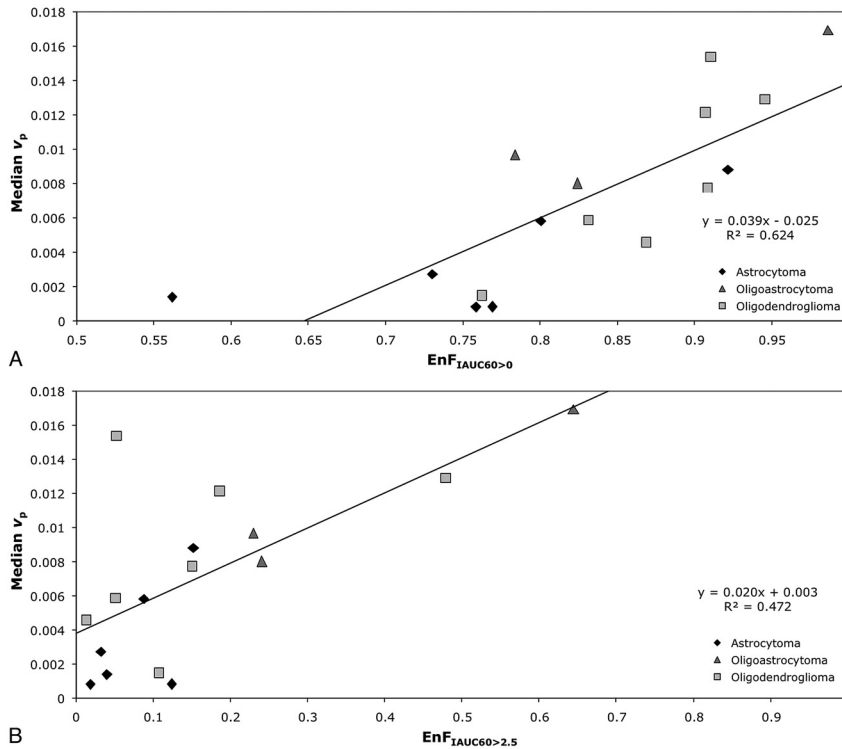


Fig 1. Scatter diagrams of EnF measures and v_p in grade II gliomas. *A*, $EnF_{IAUC60>0}$ versus median v_p . *B*, $EnF_{IAUC60>2.5}$ versus median v_p . The black diamond indicates astrocytoma; the medium gray triangle, oligoastrocytoma; and the light gray square, oligodendroglioma.

Table 2: Correlation matrix for all parameters in the grade IV glioma group and Spearman ρ correlation coefficients for cross-correlation between parameters (with significance levels)

	K^{trans}	v_e	v_p	$EnF_{IAUC60>0}$	$EnF_{IAUC60>2.5}$
K^{trans}	1.000	0.442 ($P = .031$) ^a	0.496 ($P = .014$) ^a	0.633 ($P = .001$) ^b	0.770 ($P < .0005$) ^b
v_e	0.442 ($P = .031$)	1.000	0.222 ($P = .298$)	0.097 ($P = .654$)	0.300 ($P = .154$)
v_p	0.496 ($P = .014$) ^a	0.222 ($P = .298$)	1.000	0.514 ($P = .010$) ^b	0.537 ($P = .007$) ^b
$EnF_{IAUC60>0}$	0.633 ($P = .001$) ^b	0.097 ($P = .654$)	0.514 ($P = .010$) ^b	1.000	0.870 ($P < .0005$) ^b
$EnF_{IAUC60>2.5}$	0.770 ($P < .0005$) ^b	0.300 ($P = .154$)	0.537 ($P = .007$) ^b	0.870 ($P < .0005$) ^b	1.000

^a Correlation is significant at the .05 level (2-tailed).

^b Correlation is significant at the .01 level (2-tailed).

mas (1 biopsied and 6 surgically debulked). The 3 grade III tumors were all diagnosed by surgical debulking and included 2 anaplastic astrocytomas and 1 anaplastic oligodendroglioma. The 24 grade IV gliomas included 23 glioblastoma multiformes (9 biopsied and 14 surgically debulked) and 1 gliosarcoma (surgically debulked). All 10 of the oligodendrogliomas/oligoastrocytomas in this study exhibited loss of heterozygosity of 1p/19q.

In the group of grade II tumors, $EnF_{IAUC60>0}$ correlated with v_p ($P < .0005$; Spearman rho correlation coefficient = 0.838; $R^2 = 0.6245$; Table 1 and Fig 1A), but not with K^{trans} ($P = .926$) or v_e ($P = .213$). Similarly, there was a significant correlation between $EnF_{IAUC60>2.5}$ and v_p ($P = .003$; Spearman rho correlation coefficient = 0.697; $R^2 = 0.4727$; Table 1 and Fig 1B), but not with K^{trans} ($P = .996$) or v_e ($P = .721$).

In the subgroup of grade II astrocytomas, neither $EnF_{IAUC60>0}$ or $EnF_{IAUC60>2.5}$ correlated with v_p ($P = .266$ and $P = .208$), K^{trans} ($P = .329$ and $P = .329$), or v_e ($P = .486$ and $P = .329$). In the subgroup of grade II tumors with an oligodendroglioma component, v_p correlated with both $EnF_{IAUC60>0}$ and $EnF_{IAUC60>2.5}$ ($P = .013$; Spearman rho correlation coefficient = 0.745; $R^2 = 0.604$ and $P = .048$; Spearman rho correlation coef-

ficient = 0.636; $R^2 = 0.397$), but not with K^{trans} ($P = .440$ and $P = .483$) or v_e ($P = .777$ and $P = .603$).

In grade IV tumors, $EnF_{IAUC60>0}$ correlated with both K^{trans} ($P = .001$; Spearman rho correlation coefficient = 0.633; $R^2 = 0.3501$; Table 2 and Fig 2A) and v_p ($P = .01$; Spearman rho correlation coefficient = 0.514; $R^2 = 0.1564$; Table 2 and Fig 3A), but not with v_e ($P = .654$). Again, similar relationships were seen between $EnF_{IAUC60>2.5}$ and K^{trans} ($P < .0005$; Spearman rho correlation coefficient = 0.770; $R^2 = 0.4699$; Table 2 and Fig 2B), v_p ($P = .007$; Spearman rho correlation coefficient = 0.537; $R^2 = 0.2429$; Table 2 and Fig 3B), and v_e ($P = .154$). Multiple linear regression analysis demonstrated K^{trans} as the only significant independent correlate of both $EnF_{IAUC60>0}$ ($P = .002$ and $R^2 = 0.592$) and $EnF_{IAUC60>2.5}$ ($P = .0002$ and $R^2 = 0.686$). Cross-correlation was found between K^{trans} and v_p ($P = .014$; Spearman rho correlation coefficient = 0.496; $R^2 = 0.4618$; Table 2 and Fig 4). The addition of v_p did not significantly influence the multiple linear regression model.

Discussion

This study examined the relationship between EnF and characteristics of the tumoral vascular microenvironment defined

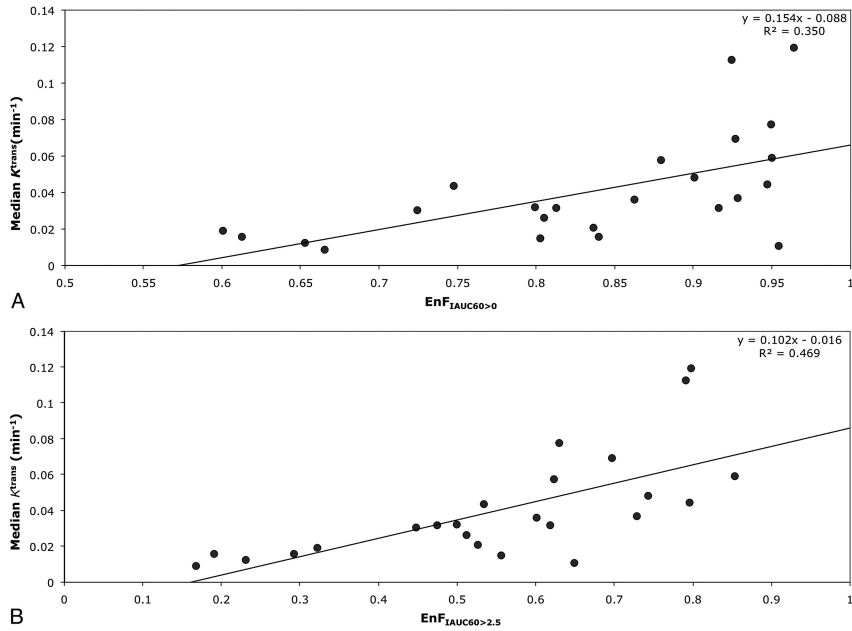


Fig 2. Scatter diagrams of EnF measures and K^{trans} in grade IV gliomas. A, $\text{EnF}_{\text{IADC60}>0}$ versus median K^{trans} . B, $\text{EnF}_{\text{IADC60}>2.5}$ versus median K^{trans} .

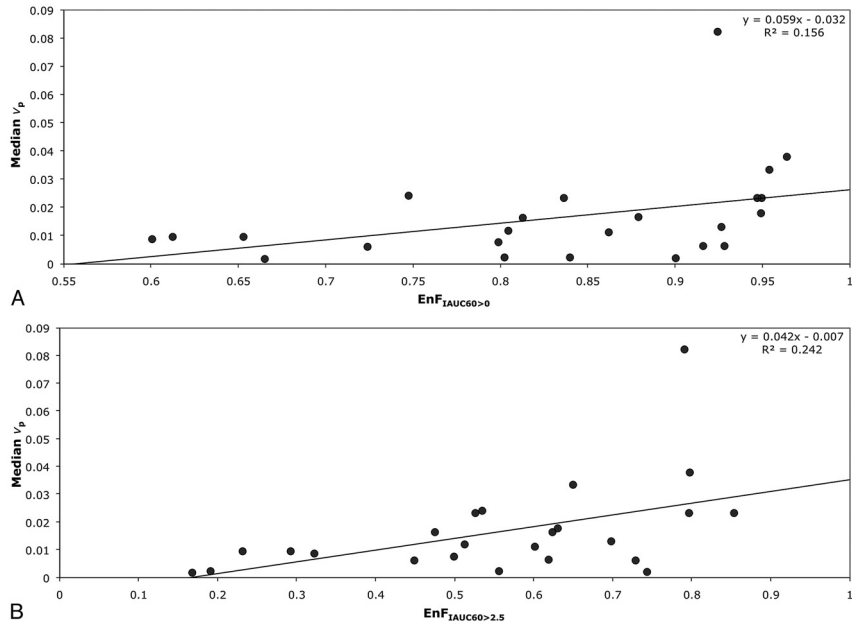


Fig 3. Scatter diagrams of EnF measures and v_p in grade IV gliomas. A, $\text{EnF}_{\text{IADC60}>0}$ versus median v_p . B, $\text{EnF}_{\text{IADC60}>2.5}$ versus median v_p .

by the model-based parameters K^{trans} , v_p , and v_e . EnF is based on the IAUC and has advantages in that it is relatively simple to perform, is unlikely to be influenced significantly by variations in scanner and sequence type, and does not rely on complex postprocessing pharmacokinetic modeling techniques.^{1,3,33} Thus, it is more suitable for use within the clinical setting and for multicenter studies because it is less reliant on the technical expertise required for more complex analysis processes.

Although EnF uses IAUC to classify pixels as enhancing or nonenhancing, it is a distinct metric with important differences from the widely used vascular biomarkers derived from DCE-MR imaging and DCE-CT. EnF will be affected by a wider range of physiologic processes. These include those that influence local IAUC in enhancing tissue and

physiologic conditions that prevent perfusion or enhancement. The volume of necrotic and of viable but inadequately perfused tissue directly contributes to the measurement. EnF will, therefore, be influenced by regional arterial-venous pressure differences and tumor interstitial pressure. In a study of ovarian and colorectal cancer treated with CDP860, a selective platelet-derived growth factor inhibitor known to cause primary decreases in tumor interstitial pressure, increases in EnF occurred rapidly after administration of the drug,²⁶ though model-based parameters, including IAUC, K^{trans} , v_e , and v_p showed no change.

Cerebral tumors develop in a unique physiologic environment in which increases in tumor volume directly affect the pressure of the compartment in which they develop. Conse-

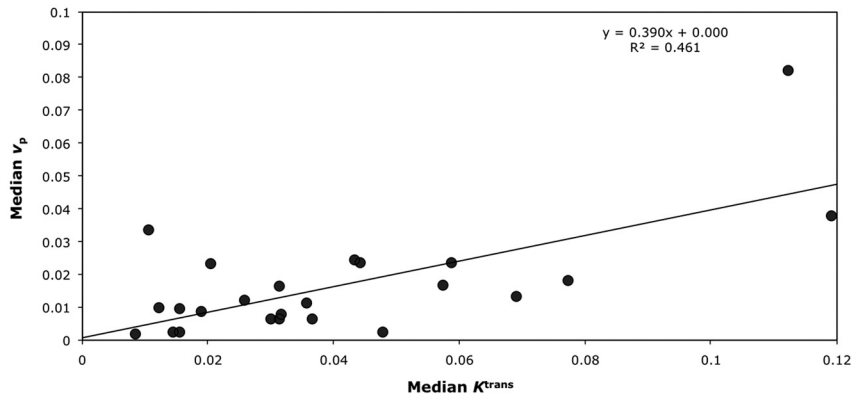


Fig 4. Scatter diagram of median K^{trans} versus median v_p in grade IV gliomas.

quently, changes in interstitial pressure, which is equivalent to intracranial pressure, directly reflect the volume and growth rate of the tumor and its components. Hence, a rapidly growing glioma may be expected to develop an interstitial pressure that exceeds perfusion pressures in the tumor core, which will consequently fail to enhance. This process will result in significant hypoperfusion and hypoxia in the central parts of the tumor. These effects will, in turn, result in release of angiogenic cytokines, particularly VEGF. Glioblastomas produce higher levels of VEGF than any other tumor, which has led to recent trials of antiangiogenic therapy, which have been associated with increased survival.^{34,35} Thus, EnF may provide novel information regarding both tumor development and therapeutic response to novel agents.

In this study, we have attempted to increase our understanding of the behavior of EnF as a putative biomarker for glioma by examining the relationship between EnF and conventional biomarkers of enhancing tumor tissue. This work confirms that EnF, both thresholded and unthresholded, may be of value as a biomarker in glioma. At presentation, it could provide a simple, robust, and model-free alternative to parameters derived from pharmacokinetic analysis of DCE-MR imaging data. The manner in which EnF relates to the DCE-MR imaging parameters depends on the features of the vascular microenvironment. In low-grade tumors, vessel permeability is low and the blood-brain barrier is essentially intact; therefore, contrast remains mostly within the vascular space and EnF correlates with v_p (Fig 1). Conversely, in high-grade tumors, there is high blood flow and local disruption of the blood-brain barrier with marked leakage of contrast into the extravascular extracellular space. In this group of tumors, both K^{trans} , which reflects flow and capillary permeability, and v_p correlate with EnF (Figs 2 and 3). However, multiple regression analysis shows that v_p is a covariate of K^{trans} (Fig 4). No correlation between EnF and v_e was found for either grade II or grade IV tumors.

In high-grade tumors, K^{trans} has been shown to predict prognosis independent of cerebral blood volume measurements.²³ At the time of analysis, survival data were not available for this group of patients; therefore, the relationship between EnF and patient outcome cannot be reported. However, if this prognostic relationship does hold for EnF, then the technique may provide a potentially important prognostic marker.

The main limitations with this study were the small num-

bers and failure to separate the grade II and III tumors according to histologic subtype. Only 3 patients had grade III gliomas (2 anaplastic astrocytomas and 1 anaplastic oligodendroglioma), making it difficult to assess how the measures of enhancement of grade III tumors behave compared with those of grade II and IV tumors. Although there were insufficient numbers for formal analysis, there was a tendency for the measures of EnF of the grade III tumors to lie among the values for grade II tumors. This poor separation of the grade III tumors from grade II tumors may reflect the histologic subtype of the grade II glioma group (predominantly oligodendrogliomas and oligoastrocytomas) or the small number of anaplastic tumors. The failure of the subanalysis of the grade II pure astrocytomas to demonstrate any correlation between v_p and either $EnF_{IAUC60>0}$ or $EnF_{IAUC60>2.5}$ most likely reflects the small number within this cohort ($n = 6$).

Conclusions

EnF is a simple, model-free, and robust metric that does not require the complex pharmacokinetic modeling necessary for calculation of v_p and K^{trans} . It is a distinct entity and influenced by a wide range of physiologic processes. However, EnF correlates with v_p in grade II glioma and K^{trans} in grade IV glioma; and given the relationships of K^{trans} and v_p to prognosis, tumor subtype, and genotype in glioma, measures of EnF have the potential to be an important adjunctive biomarker.

References

1. Evelhoch JL. Key factors in the acquisition of contrast kinetic data for oncology. *J Magn Reson Imaging* 1999;10:254–59
2. Roberts C, Issa B, Stone A, et al. Comparative study into the robustness of compartmental modeling and model-free analysis in DCE-MRI studies. *J Magn Reson Imaging* 2006;23:554–63
3. Tofts PS. Modeling tracer kinetics in dynamic Gd-DTPA MR imaging. *J Magn Reson Imaging* 1997;7:91–101
4. Aronen HJ, Gazit IE, Louis DN, et al. Cerebral blood volume maps of gliomas: comparison with tumor grade and histologic findings. *Radiology* 1994;191:41–51
5. Aronen HJ, Glass J, Pardo FS, et al. Echo-planar MR cerebral blood volume mapping of gliomas: clinical utility. *Acta Radiol* 1995;36:520–28
6. Aronen HJ, Pardo FS, Kennedy DN, et al. High microvascular blood volume is associated with high glucose uptake and tumor angiogenesis in human gliomas. *Clin Cancer Res* 2000;6:2189–200
7. Knopp EA, Cha S, Johnson G, et al. Glial neoplasms: dynamic contrast-enhanced T2*-weighted MR imaging. *Radiology* 1999;211:791–98
8. Lam WW, Chan KW, Wong WL, et al. Pre-operative grading of intracranial glioma. *Acta Radiol* 2001;42:548–54
9. Law M, Yang S, Babb JS, et al. Comparison of cerebral blood volume and

- vascular permeability from dynamic susceptibility contrast-enhanced perfusion MR imaging with glioma grade. *AJNR Am J Neuroradiol* 2004;25:746–55
10. Law M, Yang S, Wang H, et al. Glioma grading: sensitivity, specificity, and predictive values of perfusion MR imaging and proton MR spectroscopic imaging compared with conventional MR imaging. *AJNR Am J Neuroradiol* 2003;24:1989–98
 11. Lev MH, Ozsunar Y, Henson JW, et al. Glial tumor grading and outcome prediction using dynamic spin-echo MR susceptibility mapping compared with conventional contrast-enhanced MR: confounding effect of elevated rCBV of oligodendrogliomas [corrected]. *AJNR Am J Neuroradiol* 2004;25:214–21
 12. Sadeghi N, Salmon I, Decaestecker C, et al. Stereotactic comparison among cerebral blood volume, methionine uptake, and histopathology in brain glioma. *AJNR Am J Neuroradiol* 2007;28:455–61
 13. Patankar TF, Haroon HA, Mills SJ, et al. Is volume transfer coefficient (K(trans)) related to histologic grade in human gliomas? *AJNR Am J Neuroradiol* 2005;26:2455–65
 14. Ludemann L, Grieger W, Wurm R, et al. Quantitative measurement of leakage volume and permeability in gliomas, meningiomas and brain metastases with dynamic contrast-enhanced MRI. *Magn Reson Imaging* 2005;23:833–41
 15. Cha S, Tihan T, Crawford F, et al. Differentiation of low-grade oligodendrogliomas from low-grade astrocytomas by using quantitative blood-volume measurements derived from dynamic susceptibility contrast-enhanced MR imaging. *AJNR Am J Neuroradiol* 2005;26:266–73
 16. Law M, Brodsky JE, Babb J, et al. High cerebral blood volume in human gliomas predicts deletion of chromosome 1p: preliminary results of molecular studies in gliomas with elevated perfusion. *J Magn Reson Imaging* 2007;25:1113–19
 17. Jenkinson MD, Smith TS, Joyce KA, et al. Cerebral blood volume, genotype and chemosensitivity in oligodendroglial tumours. *Neuroradiology* 2006;48:703–13. Epub 2006 Aug 26
 18. Cha S, Yang L, Johnson G, et al. Comparison of microvascular permeability measurements, K(trans), determined with conventional steady-state T1-weighted and first-pass T2*-weighted MR imaging methods in gliomas and meningiomas. *AJNR Am J Neuroradiol* 2006;27:409–17
 19. Provenzale JM, Wang GR, Brenner T, et al. Comparison of permeability in high-grade and low-grade brain tumors using dynamic susceptibility contrast MR imaging. *AJR Am J Roentgenol* 2002;178:711–16
 20. Roberts HC, Roberts TP, Brasch RC, et al. Quantitative measurement of microvascular permeability in human brain tumors achieved using dynamic contrast-enhanced MR imaging: correlation with histologic grade. *AJNR Am J Neuroradiol* 2000;21:891–99
 21. Cao Y, Tsien CI, Nagesh V, et al. Survival prediction in high-grade gliomas by MRI perfusion before and during early stage of RT [corrected]. *Int J Radiat Oncol Biol Phys* 2006;64:876–85
 22. Law M, Oh S, Johnson G, et al. Perfusion magnetic resonance imaging predicts patient outcome as an adjunct to histopathology: a second reference standard in the surgical and nonsurgical treatment of low-grade gliomas. *Neurosurgery* 2006;58:1099–107
 23. Mills SJ, Patankar TA, Haroon HA, et al. Do cerebral blood volume and contrast transfer coefficient predict prognosis in human glioma? *AJNR Am J Neuroradiol* 2006;27:853–58
 24. Law M, Oh S, Babb JS, et al. Low-grade gliomas: dynamic susceptibility-weighted contrast-enhanced perfusion MR imaging—prediction of patient clinical response. *Radiology* 2006;238:658–67
 25. Law M, Young RJ, Babb JS, et al. Gliomas: predicting time to progression or survival with cerebral blood volume measurements at dynamic susceptibility-weighted contrast-enhanced perfusion MR imaging. *Radiology* 2008;247:490–98
 26. Jayson GC, Parker GJ, Mullaitha S, et al. Blockade of platelet-derived growth factor receptor-beta by CDP860, a humanized, PEGylated di-Fab', leads to fluid accumulation and is associated with increased tumor vascularized volume. *J Clin Oncol* 2005;23:973–81. Epub 2004 Oct 4
 27. Mullaitha SA, Ton NC, Parker GJ, et al. Phase I evaluation of a fully human anti-alpha v integrin monoclonal antibody (CNTO 95) in patients with advanced solid tumors. *Clin Cancer Res* 2007;13:2128–35
 28. O'Connor JP, Jayson GC, Jackson A, et al. Enhancing fraction predicts clinical outcome following first-line chemotherapy in patients with epithelial ovarian carcinoma. *Clin Cancer Res* 2007;13:6130–35
 29. Mills SJ, Soh C, O'Connor JP, et al. Tumour enhancing fraction (EnF) in glioma: relationship to tumour grade. *Eur Radiol* 2009;19:1489–98
 30. Louis DN, Ohgaki H, Wiestler OD, et al. The 2007 WHO classification of tumours of the central nervous system. *Acta Neuropathol* 2007;114:97–109. Epub 2007 Jul 6
 31. Thompson G, Cain J, Jackson A, et al. Interobserver agreement for cerebral glioma volumetrics on conventional MR imaging. In: *Proceedings of the 16th Annual Scientific Meeting and Exhibition of the International Society of Magnetic Resonance in Medicine*, Toronto, Ontario, Canada. May 3–9, 2008
 32. Parker GJM, Jackson A, Waterton JC, et al. Automated arterial input function extraction for T1-weighted DCE-MRI. In: *Proceedings of the 11th Annual Scientific Meeting and Exhibition of the International Society of Magnetic Resonance in Medicine*, Toronto, Ontario, Canada. July 10–16, 2003
 33. Parker GJM, Buckley DL. *Tracer Kinetic Modelling for T1-Weighted DCE-MRI*. Berlin: Springer-Verlag; 2005:81–92
 34. Norden AD, Young GS, Setayesh K, et al. Bevacizumab for recurrent malignant gliomas: efficacy, toxicity, and patterns of recurrence. *Neurology* 2008;70:779–87
 35. Sathornsumetee S, Reardon DA, Desjardins A, et al. Molecularly targeted therapy for malignant glioma. *Cancer* 2007;110:13–24